Journal of Applied Electrochemistry (2023) 53:1831–1842
https://doi.org/10.1007/s10800-023-01878-z

RESEARCH ARTICLE

Effect of palladium and its nanogeometry on the redox electrochemistry of tetracyanoquinodimethane modified electrode; application in electrochemical sensing of ascorbic acid

Kuldeep Kumar Maurya[1] · **Kulveer Singh**[1] · **Manisha Malviya**[1]

Received: 22 December 2022 / Accepted: 11 March 2023 / Published online: 1 April 2023

Abstract

The current work reports the effect of palladium nanoparticles and their nanogeometry on the redox electrochemistry of tetracyanoquinodimethane (TCNQ) modified electrodes. Palladium nanoparticles were prepared with different concentrations of 3-aminopropyltrimethoxysilane and calcination at 600 °C to yield PdNP-1 and PdNP-2 of the average size of 1 µm and 12 nm, respectively. The palladium nanoparticles were characterized by TEM, XRD, and AFM techniques. The electrochemical excellence of ascorbic acid was resoluted using cyclic voltammetry amperometry, electrochemical impedance spectroscopy, and differential pulse voltammetry. A limit of detection (LOD) was found to be 51.61, 44.38 and 30.10 µM over a linear range from 50 to 625 µM for modified CPE/TCNQ, CPE/TCNQ-PdNP-1, and CPE/TCNQ-PdNP-2, respectively, determined by amperometric analysis for ascorbic acid at pH 7. The synergistic effect of Palladium and π* orbital of TCNQ played an important role in the enhancement of the catalytic activity of the modified electrode. The modified electrode showed good sensitivity, stability, and reproducibility which was confirmed by cyclic voltammetry, and amperometric analysis. The charge transfer resistance value also indicated that the modified electrode hads good electrocatalytic activity.

Graphical abstract

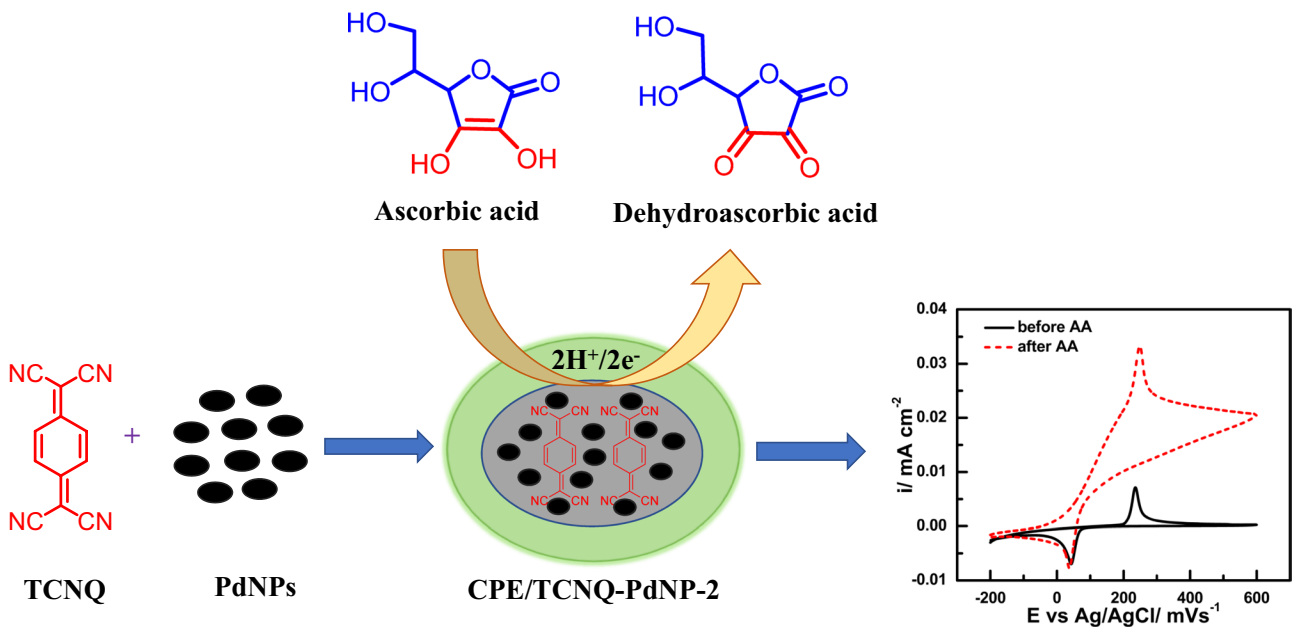

Keywords Electrocatalysis · Palladium nanoparticle · Tetracyanoquinodimethane · Differential pulse voltammetry · 3-aminopropyltrimethoxysilane

Extended author information available on the last page of the article

1 Introduction

Nanotechnology has brought about a standard shift in the essential characteristics of matter during the last few decades, leading to the creation of novel systems and materials. Nanodevices are highly sought-after on the market because of their sensitivity, low power consumption, selectivity, precision, efficiency, and fast speed [1]. As significant, though, is the development of an electrochemical sensing platform that is very sensitive, excellently selective in the attendance of other biomolecules, has a long shelf life, is stable, and exhibits minimal cytotoxicity without the use of an electron transfer mediator [2–4]. Numerous chemically modified electrodes and biosensors have been developed and successfully used in the detection of numerous biomolecules and toxic metals using a variety of electrochemical sensing techniques, including chronoamperometry, electrochemical impedance spectroscopy, cyclic voltammetry, linear sweep voltammetry, and square wave voltammetry [5, 6]. Carbon paste working electrodes have recently been incorporated into electrochemical sensors for the determination of significant electroactive molecules due to their distinctive benefits, such as enhanced electronic properties, low cost, renewability of the electrode surface, the flexibility of chemical modification, wide potential windows, and low background current [7, 8]. The use of nanomaterials in numerous sectors is expanding quickly and has promising futures. The development of sensitive and selective biosensors has benefited from recent advancements in nanotechnology [9]. The electrochemical reactivity and sensitivity of analytes can be increased by altering the electrode surface using a variety of nanostructures [10]. Redox-active sites increase the speed of electron transport by lowering its activation overpotential [11, 12]. It should be noted that because of their large surface areas, excellent electrical conductivity, and strong catalytic activity, noble metal NPs have been explored for electrochemical sensing. These metal NPs are helpful to lower the overpotentials of electrochemical sensors and keep redox reactions reversible [13, 14].

Electroanalytical techniques are valuable for gaining a thorough knowledge of multi-electron transfer systems. The electrochemistry of neurotransmitters, important biomolecules, organic (insecticides and pesticides), and inorganic materials, among others, is rife with multi-step mechanisms [10]. These techniques have a wide linear dynamic range, great sensitivity, precision, and accuracy, and need apparatus that is comparatively inexpensive. Electroanalytical investigations are more frequently utilized in industrial, and biomedical applications, drug analysis in various dosage forms, and notably in biological samples with the development of more sensitive pulse techniques [15]. Electroanalytical techniques may quickly address numerous pharmaceutical issues with great, precision, sensitivity, accuracy, and selectivity. Some of the most efficient electroanalytical methods are based on the principle of continually adjusting the applied potentials to the electrode solution contact and the consequently studied current. Electroanalytical techniques (particularly stripping analysis) are well-established as effective methods for determining trace analytes. These methods have been developed for a wide range of cations, anions, as well as organic compounds. Electrochemical methods, particularly voltammetry, have grown in prominence in recent years. These electrochemical methods have been used to identify pharmaceutical chemicals in dosage forms as well as biological samples [9].

Tetracyanoquinodimethane (TCNQ) with four cyano groups and π conjugation bonds have facilitated the formation of organic charge transfer complexes and ion-radical salts like K (TCNQ) and Na (TCNQ) [16–22]. TCNQ has also been used as a redox mediator for regenerating Oxidoreductase enzymes, especially glucose oxidase, and peroxidase, including the cofactor participating with dehydrogenase enzyme [23–27]. The advantage of the organic redox mediator is low background current even at a higher quantity within graphite paste which in turn allows sensitive and precise probing of various enzymatic reactions [28]. This justified the potential utilization of TCNQ in electrochemical biosensing. Although TCNQ has numerous advantages with electrochemical sensing, the dynamics of electrochemical reaction between biocatalyst and TCNQ is relatively slower as compared to that recorded with ferrocene derivative under similar conditions. This necessitated the search for a novel way to enhance the electrochemical performances of TCNQ as a redox mediator for a variety of practical applications on electrocatalysis, as attempted in the current study.

The redox electrochemistry of the electron transfer mediator within a heterogeneous matrix has been shown to be dependent on the support morphology. The redox electrochemistry becomes sluggish on the exploitation of a nanostructured matrix for redox molecules encapsulation [29]. The sluggish electrochemistry related to the redox mediator encapsulated nanostructured matrix is due to the restricted mobility of the redox couple within the heterogeneous phase. This directed the current study toward a possible approach to fastening the rate of bio-electrochemical interaction between enzyme and redox mediators for reliable and sensitive electrochemical sensing. Herein, an attempt was made to introduce palladium into organically modified silicate (ORMOSIL) precursors as a heterogeneous matrix, involving the active role of palladium chloride [30]. This involved a specific interaction between palladium chloride and precursors of ORMOSIL, i.e., 3-glycidoxypropyltrimethoxysilane (GPTMS) and trimethoxysilane (TMS). GPTMS

allowed the reduction of palladium chloride into palladium nanoparticles, followed by triggering the formation of palladium-linked ORMOSIL. While TMS enabled the formation of the Pd-Si-bond within the ORMOSIL matrix. These interactions between precursors of organically modified silica in the presence of ferrocene monocarboxylic acid enabled the formation of palladium-embedded ORMOSIL resulting in excellent redox electrochemistry of ORMOSIL encapsulated ferrocene derivative, and a nanostructured-heterogeneous-matrix behaving as a solid solution during electrochemical biosensing [31, 32]. However, it is required to find either analogous variation in the redox electrochemistry of TCNQ that could be recorded as a function of palladium and its nanogeometry, as studied in the current work.

In current work, the use of functional alkoxysilane, especially 3-aminopropyltrimthoxysilane (3-APTMS) which allowed controlled conversion of palladium-positive ions into palladium nanoparticles with cyclohexanone [33] and formaldehyde [34] is demonstrated. The resultant palladium nanoparticles can be calcined at the desired temperature and can be incorporated within graphite paste with TCNQ to reveal the dependence of palladium on the redox electrochemistry of TCNQ. Furthermore, the nanogeometry of palladium nanoparticles can also be controlled simply by altering the amount of 3-APTMS. Therefore, palladium nanoparticles with two different nanogeometry are prepared and employed for incorporation in graphite paste along with TCNQ for finding the dependence of palladium and its nanogeometry on redox electrochemistry of TCNQ-modified electrode. The study involvs Transmission electron microscopy, cyclic voltammetry, impedance spectroscopy, and a typical case of ascorbic acid electrochemical sensing for confirming the effect of palladium and its nanogeometry on redox electrochemistry of TCNQ-modified electrode.

2 Experimental

2.1 Materials

Tetracyanoquinodimethane (TCNQ), graphite fine powder (particle size < 20 µm), Nujol oil (density 0.838 g/ml), potassium tetrachloropalladate (II) [K_2PdCl_4] were purchased from Sigma Aldrich Chemical Co., India. Formaldehyde and ascorbic acid were purchased from Merck, India. The other reagents used were all of the analytical grades.

2.2 Synthesis of PdNPs

The synthesis of PdNPs was done by a previously reported method [33] Briefly, 100 µl ethylene glycol solution of K_2PdCl_4(20 mM) was mixed with 5 and 10 µl of 3-APTMS (10 mM) for PdNP-1 and PdNP-2, respectively. The resultant solution was mixed on a cyclo mixture followed by the addition of formaldehyde and further stirring for 10 min. The resultant product was incubated in a microwave for about one minute and centrifuged at 6000 rpm for 10 min to obtain the black color sediment. The sediment was washed two to three times and vacuum oven dried at 80 °C for 2 h.

2.3 Fabrication of modified graphite paste electrode

On graphite powder, the newly synthesized PdNP-1 and PdNP-2 were adsorbed. In order to prepare the graphite-blended PdNPs, 100 µl of PdNPs sol was mixed with 100 mg of graphite powder (molecular measure < 20 µM), and the mixture was then ultrasonically processed at 20 kHz for 20 min. The blends were allowed to stand overnight at 50 °C to allow the dissolvable to evaporate completely. To eliminate the organic components, the PdNPs adsorbed on graphite particles were calcined at 600 °C in an N_2 atmosphere. The calcined PdNP-1/ PdNP-2 altogether TCNQ, graphite powder, and binder were homogenized in a processor. Improved carbon paste electrodes (CPE) such as CPE/TCNQ, CPE/TCNQ PdNP-1, and CPE/TCNQ PdNP-2 systems are produced depending on the presence or absence of PdNPs in the active paste (Table 1). The paste surface made as discussed was physically polished on clean paper. Bioanalytical Systems provided the electrode frame utilized to construct the carbon paste electrode. An active paste of ingredients has been used to fill the electrode body, as illustrated in Table 1.

2.4 Electrochemical measurements

For electrochemical studies, an Electrochemical Workstation Model, CHI 660E Inc., TX, USA, was utilized with a three-electrode cell with a working volume of 2 ml. As the reference and auxiliary electrodes, a silver/silver chloride electrode (Orion, Beverly, MA, USA) and a Pt electrode were used. The Ag/AgCl electrode is connected to all the potentials indicated below. The working electrode is a modified CPE/TCNQ, CPE/TCNQ-PdNP-1, and CPE/TCNQ-PdNP-2 electrode. The influence of sweep rates on peak current density (j) was investigated by recording cyclic voltammograms

Table 1 Composition of mediator-modified electrode

System	TCNQ (w/w) %	PdNPs adsorption on graphite (w/w) %	Graphite (w/w) %	Nujol oil (w/w) %
TCNQ	4.2	–	70.8	25
TCNQ-PdNP-1	4.2	10	60.8	25
TCNQ-PdNP-2	4.2	10	60.8	25

at various sweep rates ranging from 1 mV s^{-1} to 500 mV s^{-1} the absence and presence of Ascorbic acid, and amperometry in a 0.1 M phosphate buffer (pH 7.0).

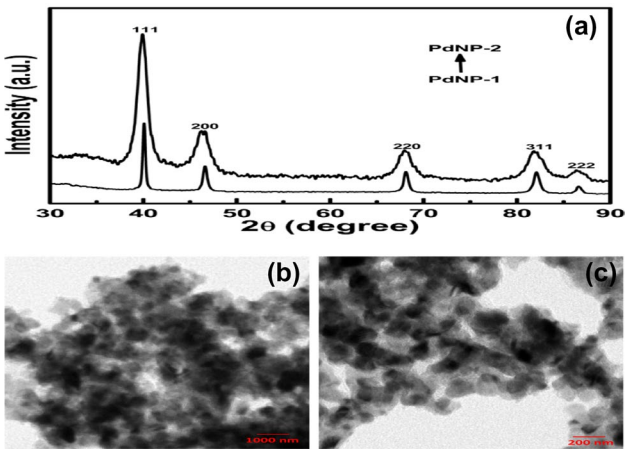

Fig. 1 Characterization of palladium nanoparticles; **a** XRD spectrum for plane and size analysis; TEM image of **b** PdNP-1 and **c** PdNP-2 for particle size analysis

3 Results and discussion

3.1 Synthesis and characterization of palladium nanoparticles

The current study revealed the preparation of nanosized palladium particles, i.e., PdNP-1 and PdNP-2 of varying size with different concentrations of 3-APTMS. The XRD spectrum as shown in Fig. 1a confirmed the planes of palladium assigned to 2θ values as per JCPDS #87–0641, corresponding to 40.02° (111), 46.49° (200), 68.05° (220), 81.74° (311), and 86.24° (222). The sharp peaks were observed for larger-size palladium nanoparticles, while the broader peaks were for smaller-size PdNPs. TEM analysis of TCNQ-PdNPs is shown in Fig. 1b and c which resemble the eventually distributed nanospheres of an average size of 1 µm and about 12 nm, respectively.

The AFM images of PdNP-1 and PdNP-2 are illustrated in Fig. 2a–c and 2d–f, respectively. The average grain size of PdNP-1 and PdNP-2 is found to be 1 and 0.2 µm, respectively. These nanoparticles are used to mix with TCNQ for making modified electrodes, namely TCNQ-PdNP-1 and

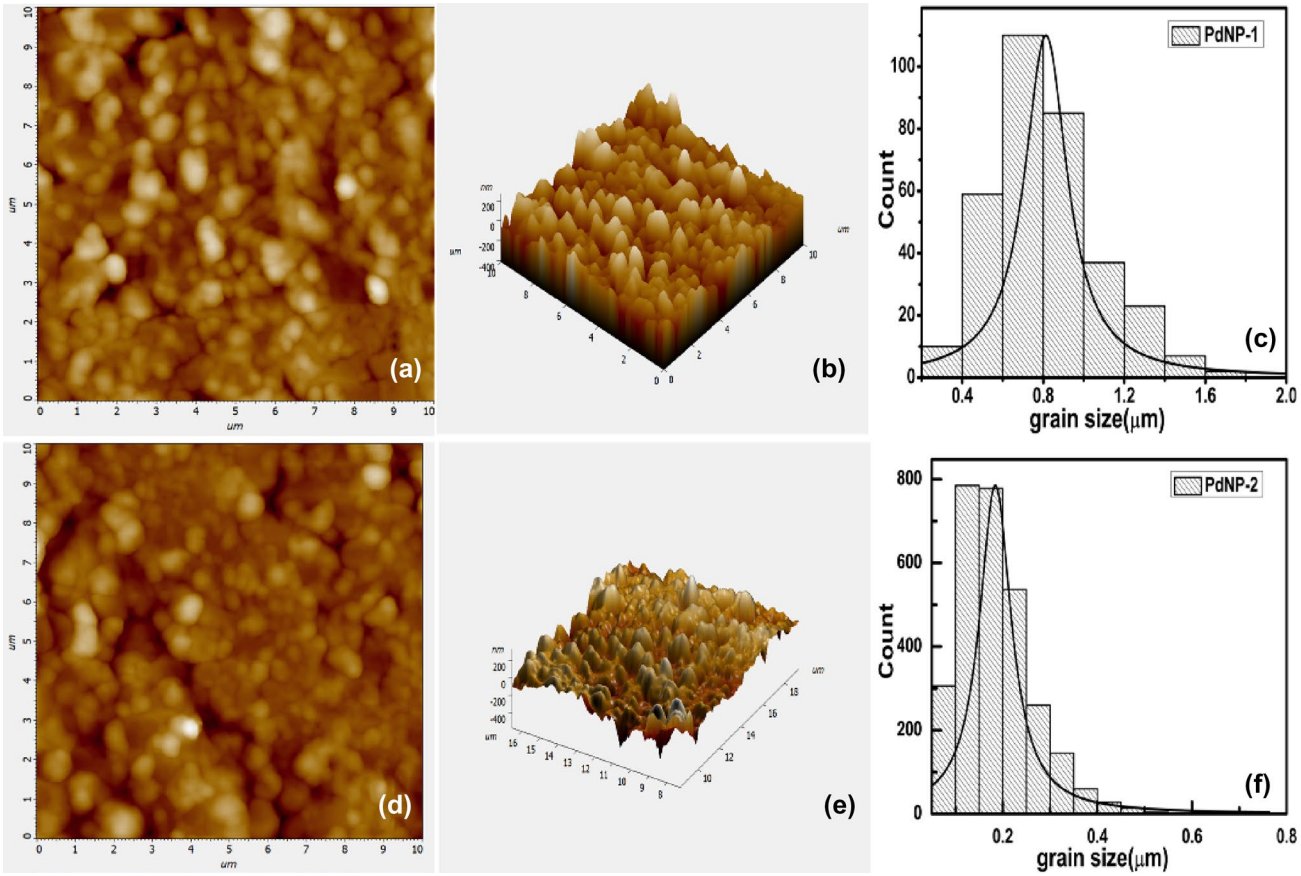

Fig. 2 **a, d** 2D AFM image, **b, e** 3D image together **c, f** histogram of PdNP-1 & PdNP-2, respectively

TCNQ-PdNP-2 for studying the impact of PdNPs on the redox electrochemistry of TCNQ.

3.2 Impact of Pd-nanogeometry on the redox electrochemistry of TCNQ-modified electrodes

After carefully adsorbing PdNP-1 and PdNP-2 on graphite powder, 3-APTMS stabilized nanoparticles were calcined at 600° C to remove all organic parts present on the Palladium nanoparticle. Calcinated nanoparticles were subsequently used to understand the impact of PdNPs on the electrochemistry of TCNQ-modified electrodes as a close contact of PdNPs and TCNQ within graphite paste may facilitate the charge transfer rate during electrochemical measurements. In this regard, interesting findings were recorded. Figure 3 illustrated the results of cyclic voltammetry of (a) CPE/TCNQ, (b) CPE/TCNQ-PdNP-1, and (c) CPE/TCNQ-PdNP-2 within the carbon paste electrode (CPE). Firstly, the variation in the redox performance of TCNQ within the CPE as a response to incorporated calcined PdNP-1 and PdNP-2 was investigated. Figure 3 also showed the cyclic voltammetry of CPE/TCNQ, CPE/TCNQ-PdNP-1, and CPE/TCNQ-PdNP-2 electrodes at different scan rates. The results justified the decrease in anodic (Epa) and cathodic (Epc) peak potentials from 243 to 231 mV. Furthermore, the anodic and cathodic peak currents were steadily raised under similar conditions indicating the reduction of charge transfer resistance as a function of palladium nanogeometry**,** further confirmed by impedance spectroscopy as in vide infra.

Subsequently, the dynamic electrochemistry was investigated based on cyclic voltammetry (CV) and differential pulse voltammetry (DPV) in the absence, and the presence of varying concentrations of ascorbic acid as efficient electroactive species for direct and mediated electrochemistry. The results, as shown in Fig. 4, clearly revealed the significant enhancement of anodic current attributed to the

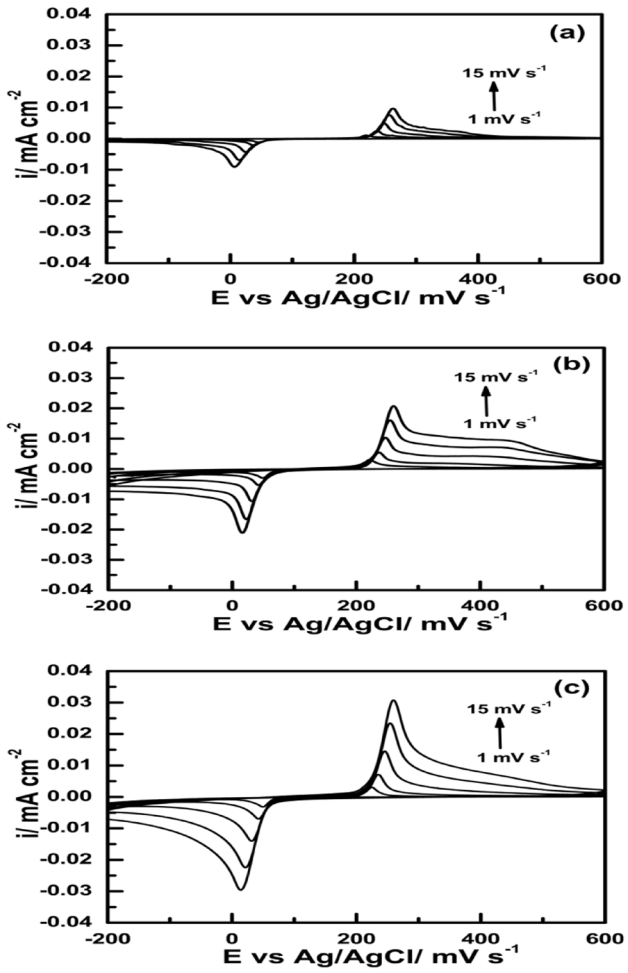

Fig. 3 Cyclic voltammetry of CPE/TCNQ (**a**) CPE/TCNQ-PdNP-1 (**b**) CPE/TCNQ-PdNP-2 (**c**) in 01. M phosphate buffer between −0.2 and 0.6 V vs Ag/AgCl at different scan rates

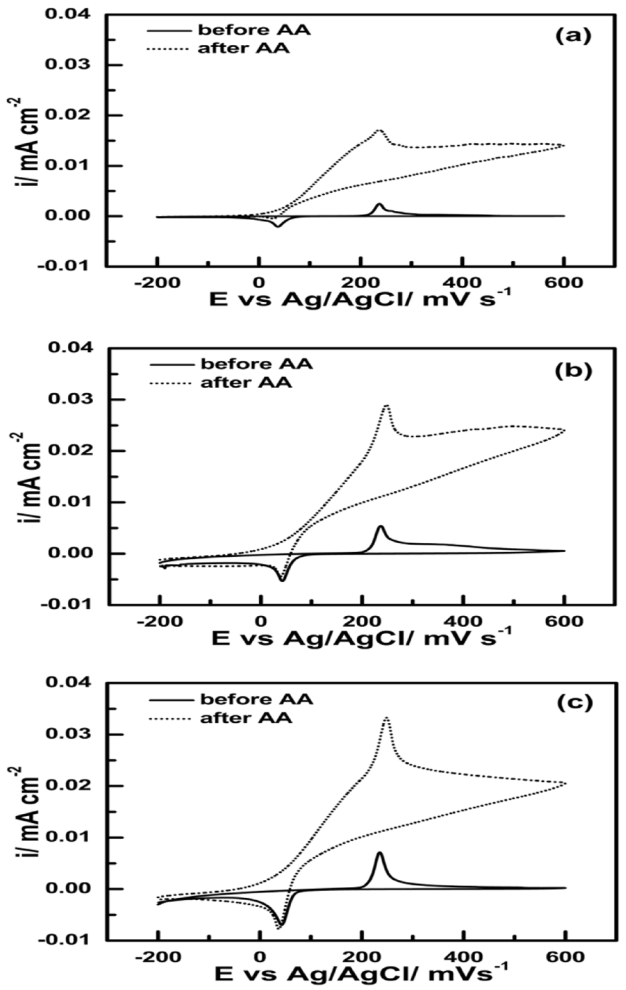

Fig. 4 Cyclic voltammograms before (solid line) and after (dotted line) addition of ascorbic acid (10 mM) for CPE/TCNQ (**a**) CPE/TCNQ-PdNP-1 (**b**) and CPE/TCNQ-PdNP-2 (**c**) electrodes

electrochemical transformation of ascorbic acid which in turn confirmed the reduction in charge transfer resistance as a function of palladium nanogeometry.

Differential pulse voltammetry (DPV) of CPE/TCNQ, CPE/TCNQ-PdNP-1, and CPE/TCNQ-PdNP-2 electrodes were subsequently investigated to understand the impact of palladium and its nanogeometry during electrochemical sensing. Figure 5a–c shows the differential pulse voltammograms at varying concentrations of ascorbic acid. The calibration curves made between peak currents of the pulse voltammogram as a function of ascorbic acid are shown in Fig. 5d. A straight-line association was obtained between the differential pulse voltammetry current and AA concentration with a gradual increase in sensitivity of AA sensing and found to be 1.5, 1.9, and 2.5 µA/mM for CPE/TCNQ, CPE/TCNQ-PdNP-1, and CPE/TCNQ-PdNP-2 electrodes, respectively, again confirming the contribution of palladium and its nanogeometry.

The finding recorded in Fig. 5 was further examined on reliable electrochemical sensing of ascorbic acid based on static electrochemistry at a constant potential close to the redox potential of CPE/TCNQ, CPE/TCNQ-PdNP-1, and CPE/TCNQ-PdNP-2 electrodes. Electroanalytical performances of modified electrodes were performed by amperometric measurement under stirring conditions. Amperometric measurement was performed successively by adding ascorbic acid (50–625 µM) to the continuously stirred solution with a working potential of 0.22 V vs Ag/AgCl and recorded. CPE/TCNQ-PdNP-2 showed higher responses than CPE/TCNQ-PdNP-1 and CPE/TCNQ-modified electrodes, as shown in Fig. 6a–c. The standard curve for ascorbic acid (AA) detection by amperometry was constructed (Fig. 6d). The outcomes imply an extensive linear association between the amperometric current and AA concentration. The limit of detection (LOD) was calculated using the following formula.

$$\mathrm{LOD} = \frac{3 \times \mathrm{S}}{\mathrm{m}}$$

where S is the standard deviation in the intercept and m is the slope of the calibration curve. The LOD were determined to be 51.61, 44.38, and 30.10 µM for CPE/TCNQ, CPE/TCNQ-PdNP-1, and CPE/TCNQ-PdNP-2 modified electrodes, respectively. [6] The sensitivity for AA sensing was

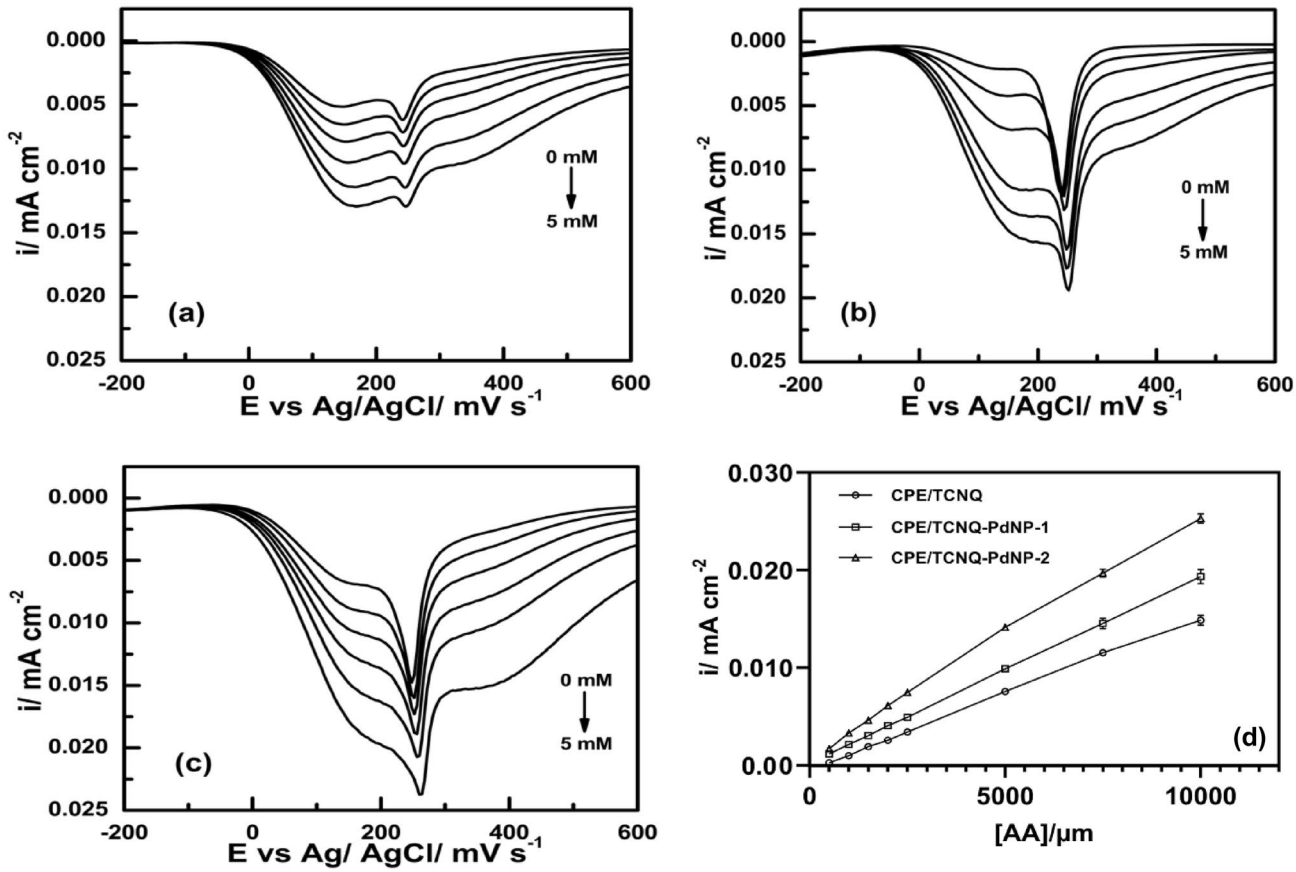

Fig. 5 Differential pulse voltammetry of CPE/TCNQ (**a**) CPE/TCNQ-PdNP-1 (**b**) CPE/TCNQ-PdNP-2 (**c**) in the presence of varying concentrations of ascorbic acid. **d** Shows the linear relation between peak current vs Concentration of ascorbic acid

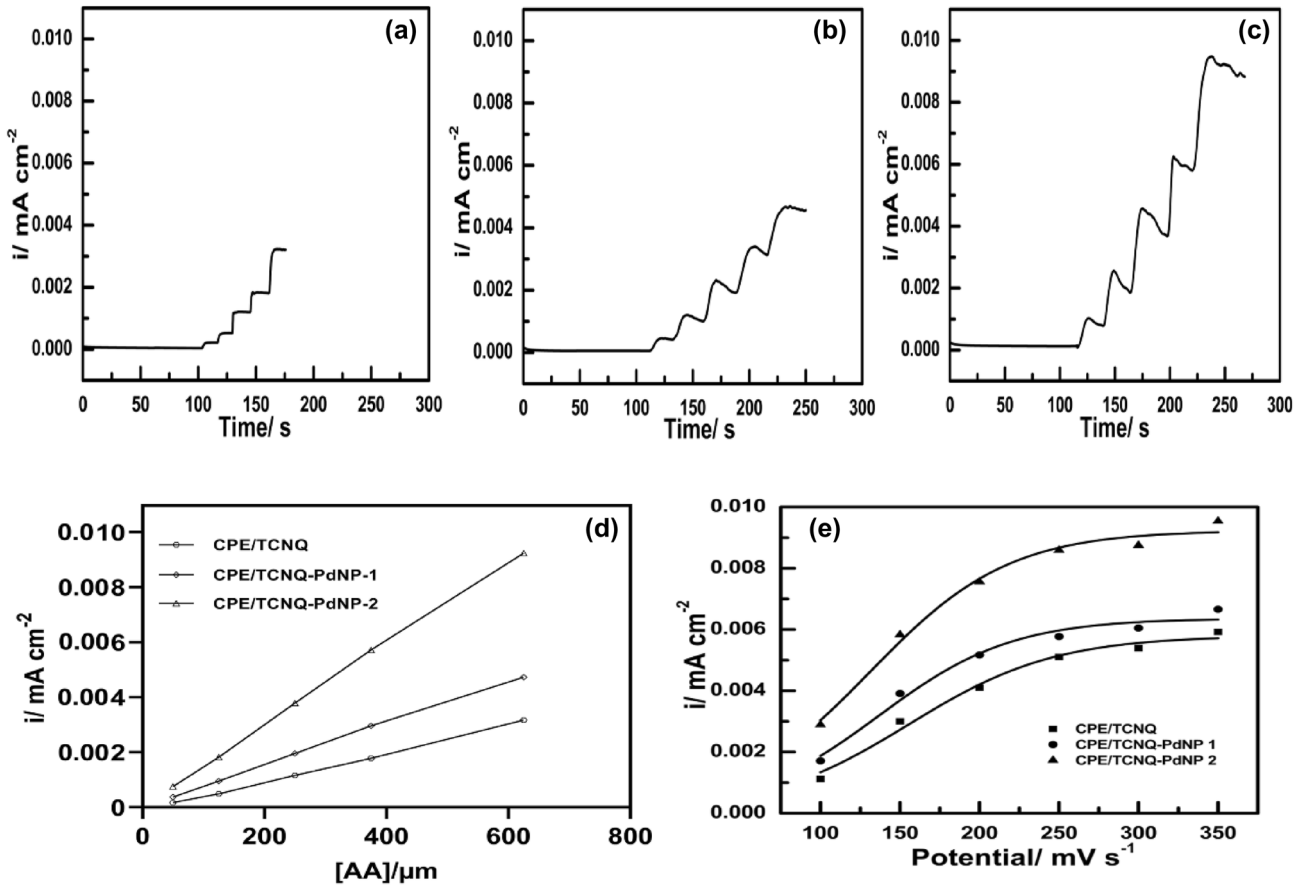

Fig. 6 Amperometric response of CPE/TCNQ (**a**) CPE/TCNQ-PdNP-1 (**b**) and CPE/TCNQ-PdNP-2 (**c**) on the addition of varying concentrations of ascorbic acid between (50 µM to 625 µM). recorded at a constant potential of 220 mV vs Ag/AgCl; (**d**) Calibration curve for ascorbic acid analysis using CPE/TCNQ (1) CPE/TCNQ-PdNP-1 (2) & CPE/TCNQ-PdNP-2 (3) system; (**e**) Chronopotentiometry of CPE/TCNQ (1) CPE/TCNQ-PdNP-1 (2) & CPE/TCNQ-PdNP-2 (3) recorded at a different operating potential between 100 to 300 mV vs Ag/AgCl

found to be 0.005, 0.0075, and 0.0148 mA/mM for CPE/TCNQ, CPE/TCNQ-PdNP-1, and CPE/TCNQ-PdNP-2 electrodes, respectively. This confirms the role of palladium and its nanogeometry on electroanalysis, further confirmed by amperometric responses recorded at varying operating potentials between 100 and 300 mV vs silver/silver chloride (Fig. 6e). This method can be efficiently used for real-time analysis of ascorbic acid in marketed formulations (Supplementary 1).

The finding of Figs. 3 and 4 may further be examined to understand the impact of palladium and its nanogeometry based on the change of the current function, which $i_p/s^{1/2}$ as a function of scan rate, and recorded in Fig. 7a–c. The results on the change of current function on scan rate in all three cases CPE/TCNQ, CPE/TCNQ-PdNP-1, and CPE/TCNQ-PdNP-2 electrodes in the absence of ascorbic acid show a horizontal straight-line, whereas on the addition of ascorbic the current function gradually decreases as an increase in scan rate and finally tend to a straight-line. The current function attains a steady value at a relatively higher scan rate in CPE/TCNQ-PdNP-2 as compared to CPE/TCNQ-PdNP-1 and CPE/TCNQ justifying faster charge transfer dynamics as a function of palladium nanogeometry.

3.3 Electrochemical impedance spectroscopy

EIS studies were additionally executed to examine the impact of change on the charge transfer characteristics and recorded for CPE/TCNQ, CPE/TCNQ-PdNP-1, and CPE/TCNQ-PdNP-2 electrodes in 0.1 M phosphate buffer between the frequency range of 1 Hz to 1000 kHz as shown in Fig. 8. A typical Nyquist plot for Randle's circuit has two parts: the semi-circular and the linear element. At low frequencies, the linear element represents the mass transfer diffusion, whereas, at high frequencies, the semicircle's diameter signifies the charge transfer resistance (Rct) [35].

The diameter of the circle component inside the Nyquist plot represents the charge transfer resistance

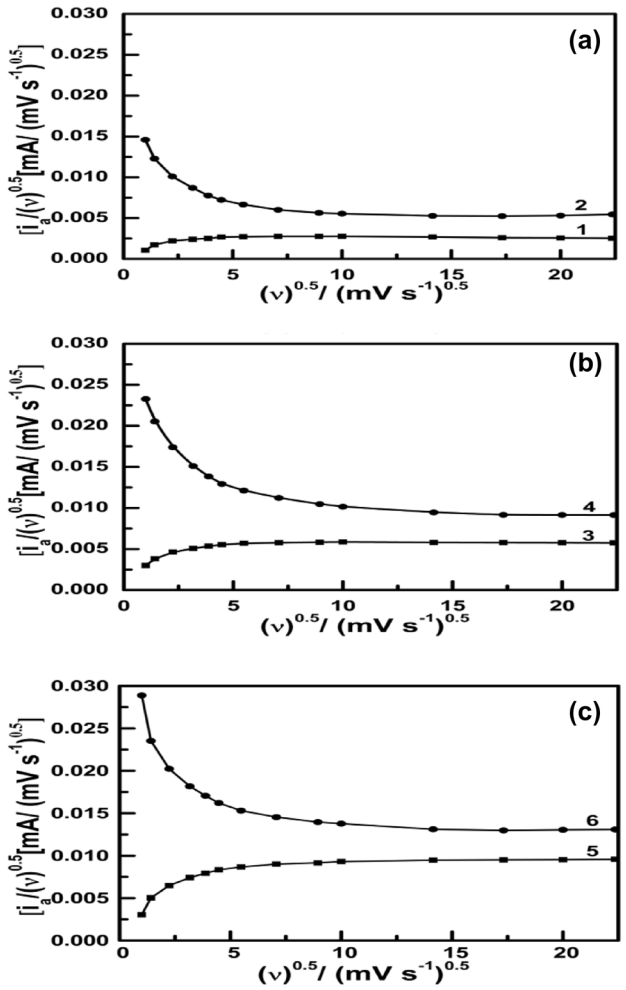

Fig. 7 The plot of current function vs square root of scan rate of CPE/TCNQ (**a**) CPE/TCNQ-PdNP-1 (**b**) and CPE/TCNQ-PdNP-2 (**c**)

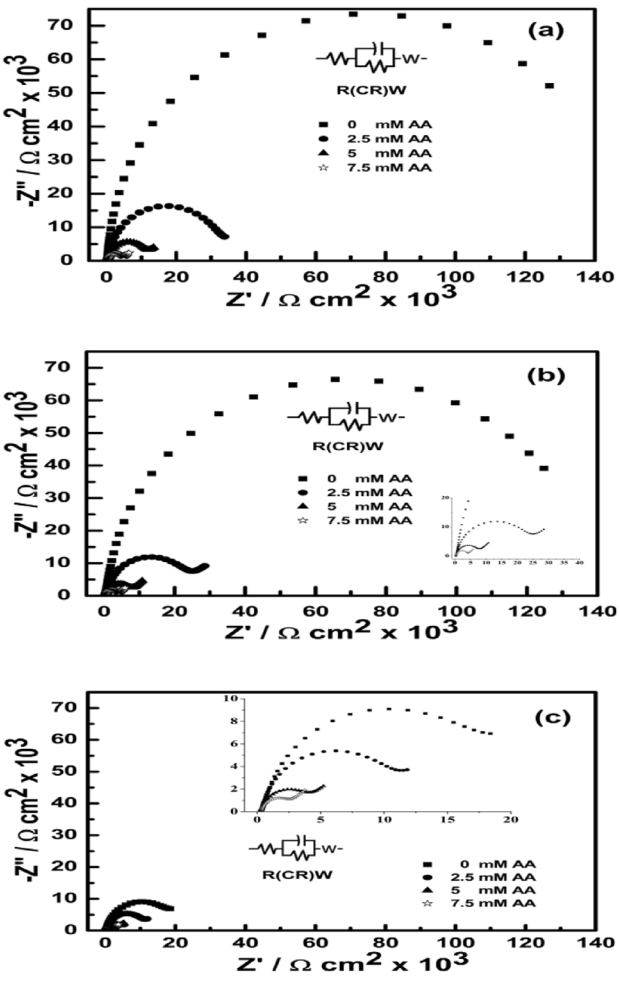

Fig. 8 **a** Nyquist plot of CPE/TCNQ (1) without adding AA (2) 2.5 mM (3) 5 mM (4) 7.5 mM. **b** CPE/TCNQ-PdNP-1 (1) without adding AA (2) 2.5 mM (3) 5 mM (4) 7.5 mM and **c** CPE/TCNQ-PdNP-2 (1) without adding AA (2) 2.5 mM (3) 5 mM (4) 7.5 mM

(Rct) of the system. CPE/TCNQ-PdNP-2 shows reduced Rct (22.15×10^3) with respect to the CPE/TCNQ-PdNP-1 (130×10^3) and CPE/TCNQ (150×10^3), respectively, which indicates that the maximum charge transfer takes place in the system CPE/TCNQ-PdNP-2. Additionally, with an increase in the concentration of ascorbic acid, the diameter of the circle decreases, and so does the gradual increase in the charge transfer process. The values of charge transfer resistance for CPE/TCNQ, CPE/TCNQ-PdNP-1, and CPE/TCNQ-PdNP-2 electrodes were calculated as recorded in Table 2, clearly justifying the impact of palladium and its nanogeometry on the redox electrochemistry of TCNQ confirming that an increase in palladium nanogeometry subsequently decreases the charge transfer resistance allowing faster dynamic electrochemistry of TCNQ-modified electrode (Table 3).

Table 2 Charge transfer resistance

Concentration of AA	TCNQ R_{ct}	TCNQ-PdNP$_1$ R_{ct}	TCNQ-PdNP$_2$ R_{ct}
Blank	150×10^3	135×10^3	22.15×10^3
3.75 mM	32×10^3	25.18×10^3	11.37×10^3
7.5 mM	11.66×10^3	8.85×10^3	4.03×10^3
11.25 mM	5.66×10^3	4.55×10^3	2.73×10^3

3.3.1 Calculation of electrochemical active surface area

The electrochemical active surface area (EASA) of working electrodes was investigated by taking cyclic voltammograms (CVs) of CPE/TCNQ, CPE/TCNQ-PdNP-1, and CPE/TCNQ-PdNP-2 in 0.1 M phosphate buffer at a scan rate of 15 mV, which is shown in Fig. 3a–c, respectively.

Table 3 Comparison of our proposed modified carbon paste electrodes with other published ascorbic acid sensors

Electrode	Linear range (μM)	LOD (μM)	Sensitivity (μA/mM)	References
MnFe2O4/MoS2/SPCE	200–1000	175	–	[36]
ERGO/GCE	500–2000	250	–	[37]
GO-TmPO4/GCE	100–1000	39	12.39	[38]
PANI/SPE	30–270	30	17.7	[39]
NiHCF/Au	100–12,000	25	–	[40]
PrGO/PB/GCE	283–2330	34.7	–	[41]
ZnO-CuxO-PPy/GCE	200–1000	25	–	[42]
CPE/TCNQ	50–625	51.61	5	This work
CPE/TCNQ-PdNP-1	50–625	44.38	7.5	This work
CPE/TCNQ-PdNP-2	50–625	30.35	14.8	This work

Peak current improved with increasing scan rate, and the related linearity graph was found. This represents the anodic and cathodic peak current vs the square root of the scan rate. To determine the EASA of CPE/TCNQ, CPE/TCNQ-PdNP-1, and CPE/TCNQ-PdNP-2, we utilized the Randles–Sevcik equation [3] described in Eq. (1).

$$Ip = 2.69 \times 10^5 n^{3/2} A D^{1/2} v^{1/2} C_0 \quad (1)$$

here A denotes the Electrochemical active surface area (cm^2), D denotes the diffusion coefficient ($cm^2\ s^{-1}$), C_0 denotes the concentration of electroactive analyte, n denotes the number of electrons exchanged during the reversible reaction, Ip denotes peak current (A), and υ denotes the scan rate (Vs^{-1}). By putting these values in Eq. (1) The EASA of CPE/TCNQ, CPE/TCNQ-PdNP-1, and CPE/TCNQ-PdNP-2 were calculated to be 0.0547, 0.2350, and 0.2704 cm^2, respectively. The electrochemical characterizations indicate that CPE/TCNQ-PdNP-2 has superior electrochemical behavior than CPE/TCNQ and CPE/TCNQ-PdNP-1. It is predicted that CPE/TCNQ-PdNP-2 to be a good platform for the electrochemical sensing of ascorbic acid.

3.3.2 Effect of pH

The pH parameter is extremely important for the electrochemical sensing of AA since it strongly influences the oxidation process. Here Fig. 9a shows the graph between current vs pH. This was confirmed by changing the pH of the control sample from 5 to 9 for AA. At pH 7.0 highest current was found thereafter either the pH value increased or the decreased value of the current decreased.

3.3.3 Reproducibility and stability

To determine the sensor's reproducibility, Five TCNQ-PdNPs/CPE-modified electrodes were produced in the same manner. Using these electrodes, anodic peak currents of 0.5 mM AA were measured. This measurement showed a relative standard deviation (RSD) of 2.0%, indicating that the modified electrode made using this procedure is showing good reproducibility. After storing the produced sensor at ambient temperature for 5, 10, and 15 days, the oxidative peak current of AA maintained 98, 96, and 94% of its original value, indicating good stability. As a result, CPE/TCNQ-PdNP-2 is projected to be employed in the detection of AA

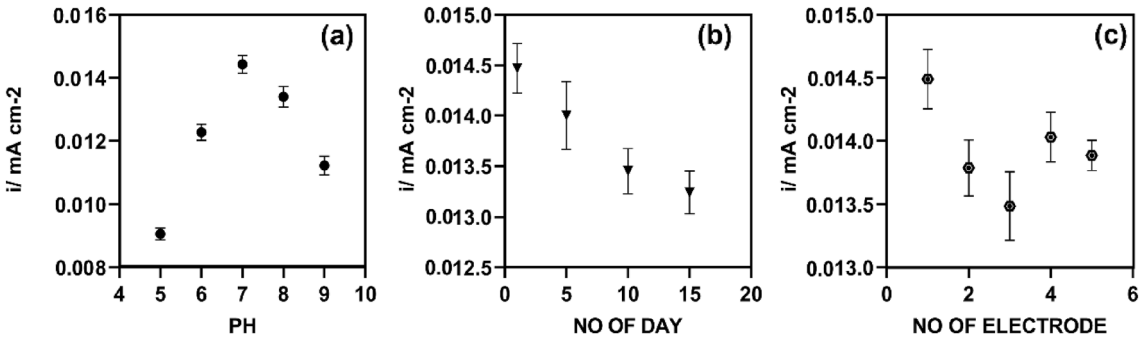

Fig. 9 **a** pH, **b** stability, and **c** reproducibility of CPE/TCNQ-PdNP-2 modified electrode

with good stability and reproducibility which is shown in Fig. 9b and 9c, respectively.

4 Conclusions

The current research was undertaken to fasten the dynamic electrochemistry of TCNQ in electrochemical sensing in the presence of palladium in two different nanogeometry. The three different systems, namely CPE/TCNQ, CPE/TCNQ-PdNP-1, and CPE/TCNQ-PdNP-2 electrodes, clearly predict the gradual decrease in charge transfer resistance as a function of palladium nanogeometry. The sluggish electrochemistry of TCNQ-modified electrodes tends to be faster in the presence of palladium, with a gradual increase in terms of peak current as a function of palladium nanogeometry. The TCNQ-modified electrode function was observed to be dependent on palladium nanogeometry even at a faster scan rate. Therefore, palladium and its nanogeometry have a significant effect in redox-mediated electrochemistry along with the introduction of electrocatalysis during electrochemical sensing/biosensing.

Supplementary Information The online version contains supplementary material available at https://doi.org/10.1007/s10800-023-01878-z.

Acknowledgements We are grateful to Central Instrumentation Facility Centre (CIFC) IIT (BHU) for providing TEM and AFM facilities. The author is also thankful to Prof. P. C. Pandey for providing an electrochemical workstation and the Head of the Department for providing other facilities.

Author contributions KKMhas done all the experimental work as well as written and revised the manuscript, KS has done the analysis of images and MM has reviewed and rewritten the manuscript.

Declarations

Conflict of interest The authors disclose that they do not have any competing interests.

References

1. Ganesh PS, Kim SY (2022) Electrochemical sensing interfaces based on novel 2D-MXenes for monitoring environmental hazardous toxic compounds: a concise review. J Ind Eng Chem 109:52–67. https://doi.org/10.1016/j.jiec.2022.02.006
2. Elugoke SE, Fayemi OE, Adekunle AS, Ganesh PS, Kim SY, Ebenso EE (2023) Sensitive and selective neurotransmitter epinephrine detection at a carbon quantum dots/copper oxide nanocomposite. J Electroanal Chem 929:117–120. https://doi.org/10.1016/j.jelechem.2022.117120
3. Rajaji U, Ganesh PS, Chen SM, Govindasamy M, Kim SY, Alshgari RA, Shimoga G (2021) Deep eutectic solvents synthesis of perovskite-type cerium aluminate embedded carbon nitride catalyst: high-sensitive amperometric platform for sensing of glucose in biological fluids. J Ind Eng Chem 102:312–320. https://doi.org/10.1016/j.jiec.2021.07.015
4. Chadchan KS, Teradale AB, Ganesh PS, Das SN (2022) Simultaneous sensing of mesalazine and folic acid at poly (murexide) modified glassy carbon electrode surface. J Mater Chem Phys 290:126–538. https://doi.org/10.1016/j.matchemphys.2022.126538
5. Okpara EC, Fayemi OE, Sherif ESM, Ganesh PS, KumaraSwamy BE, Ebenso EE (2022) Electrochemical evaluation of Cd^{2+} and Hg^{2+} ions in water using ZnO/Cu2ONPs/PANI modified SPCE electrode. Sens Bio-Sens Res 35:100476. https://doi.org/10.1016/j.sbsr.2022.100476
6. Rajaji U, Ganesh PS, Kim SY, Govindasamy M, Alshgari RA, Liu TY (2022) MoS2 sphere/2D S-Ti3C2 MXene nanocatalysts on laser-induced graphene electrodes for hazardous aristolochic acid and roxarsone electrochemical detection. ACS Appl Nano Mater 5(3):3252–3264. https://doi.org/10.1021/acsanm.1c03680
7. Ganesh PS, Teradale AB, Kim SY, Ko HU, Ebenso EE (2022) Electrochemical sensing of anti-inflammatory drug mesalazine in pharmaceutical samples at polymerized-congo red modified carbon paste electrode. Chem Phys Lett 806:140043. https://doi.org/10.1016/j.cplett.2022.140043
8. Ganesh PS, Kim SY, Kaya S, Salim R (2022) An-experimental and theoretical approach to electrochemical sensing of environmentally hazardous dihydroxy benzene isomers at polysorbate modified carbon paste electrode. Sci Rep 12(1):2149
9. Beitollahi H, Dourandish Z, Tajik S, Sharifi F, Jahani PM (2022) Electrochemical sensor based on Ni-co layered double hydroxide hollow nanostructures for ultrasensitive detection of Sumatriptan and naproxen. Biosensors 12(10):872. https://doi.org/10.3390/bios12100872
10. Beitollahi H, Tajik S, Dourandish Z, Nejad FG (2022) Simple preparation and characterization of hierarchical flower-like NiCo2O4 nanoplates: applications for sunset yellow electrochemical analysis. Biosensors 12(11):912. https://doi.org/10.3390/bios12110912
11. Beitollahi H, Tajik S, Aflatoonian MR, Makarem A (2022) A sensitive Cu (salophen) modified screen-printed electrode for simultaneous determination of dopamine and uric acid. J Electrochem Sci Eng 12(1):199–208. https://doi.org/10.5599/jese.1231
12. Beitollahi H, Tajik S, Aflatoonian MR, Makarem A (2022) Glutathione detection at carbon paste electrode modified with ethyl 2-(4-ferrocenyl- [1, 2, 3] triazol-1-yl) acetate, ZnFe2O4nano-particles, and ionic liquid. J Electrochem Sci Eng 12(1):209–217. https://doi.org/10.5599/jese.1230
13. Tajik S, Orooji Y, Ghazanfari Z, Karimi F, Beitollahi H, Varma RS, Jang HW, Shokouhimehr M (2021) Nanomaterials modified electrodes for electrochemical detection of Sudan I in food. J Food Measurement Characterization 15:3837–3852. https://doi.org/10.1007/s11694-021-00955-1
14. Moghaddam HM, Beitollahi H, Tajik S, Janani S, Khabazzadeh H, Alizadeh R (2017) Voltammetric determination of droxidopa in the presence of carbidopa using a nanostructured base electrochemical sensor. Russ J Electrochem 53:452–460. https://doi.org/10.1134/S1023193517050123
15. Faraghly OA, Hameed RSA, Alhakeem A, Nawwas HA (2014) Review analytical application using modern electrochemical techniques. Int J Electrochem Sci 9:3287–3318
16. Wang H, Qiong Wu, Wang Y, Lv X, Wang H-G (2022) A redox-active metal–organic compound for lithium/sodium-based dual-ion batteries. J Colloid Interface Sci 606:1024–1030. https://doi.org/10.1016/j.jcis.2021.08.113
17. Murthy ASN, Anita (1994) Electrochemical oxidation of L-ascorbic acid on 7,7,8,8-tetracyanoquinodimethane (TCNQ)modified electrode. Biosens Bioelectron 9:439–444. https://doi.org/10.1016/0956-5663(94)90032-9
18. Hussain Z, Zou W, Murdoch BJ, Nafady A, Field MR, Ramanathan R, Bansal V (2020) Metal-organic charge transfer complexes

of Pb (TCNQ)2 and Pb (TCNQF4)2 as new catalysts for electron transfer reactions. Adv. Mater. Interfaces 7:2001111. https://doi.org/10.1002/admi.202001111
19. Peng H, Huang S, Tranca D, Richard F, Baaziz W, Zhuang X, Samorì P, Ciesielski A (2021) Quantum capacitance through molecular infiltration of 7,7,8,8-tetracyanoquinodimethane in metal−organic framework/covalent organic framework hybrids. ACS Nano 15:18580–18589. https://doi.org/10.1021/acsnano.1c09146
20. Fujihara Y, Kobayashi H, Takaishi S, Tomai T, Yamashita M, Honma I (2020) Electrical conductivity-relay between organic charge-transfer and radical salts toward conductive additive-free rechargeable battery. ACS Appl Mater Interfaces 12:25748–25755. https://doi.org/10.1021/acsami.0c03642
21. Leith GA, Rice AM, Yarbrough BJ, Berseneva AA, Ly RT, Buck CN III, Chusov D et al (2020) A dual threat: redox-activity and electronic structures of well-defined donor–acceptor fulleretic covalent-organic materials. Angew Chem 132(15):6056–6062. https://doi.org/10.1002/ange.201914233
22. Murase R, Hudson TA, Aldershof TS, Nguyen KV, Gluschke JG, Kenny EP, Zhou X, Wang T, van Koeverden MP, Powell BJ, Micolich AP, Abrahams BF, D'Alessandro DM (2022) Multi-redox responsive behavior in a mixed-valence semiconducting framework based on bis-[1,2,5]-thiadiazolotetracyanoquinodimethane. J Am Chem Soc 144:13242–13253. https://doi.org/10.1021/jacs.2c03794
23. Ivanov I, Vidakovic-Koch T, Sundmacher K (2013) Alternating electron transfer mechanism in the case of high-performance tetrathiafulvalene–Tetracyanoquinodimethane enzymatic electrodes. J Electroanaly Chem 690:68–73. https://doi.org/10.1016/j.jelechem.2012.11.009
24. Sato R, Kawamoto T, Mori T (2019) Asymmetrical hole/electron transport in donor-acceptor mixed-stack cocrystals. J. Mater. Chem. C 7:567–577. https://doi.org/10.1039/C8TC05190A
25. Wu H, Tian C, Song X, Liu C, Yang D, Jiang Z (2013) Methods for the regeneration of nicotinamide coenzymes. Green Chem 15(7):1773–1789. https://doi.org/10.1039/C3GC37129H
26. Pandey PC, Pandey V, Mehta S (1994) An amperometric enzyme electrode for lactate based on graphite paste modified with Tetracyanoquinodimethane. Biosens Bioelectron 9:365–372. https://doi.org/10.1016/0956-5663(94)80037-5
27. Pandey PC, Pandey V, Mehta S (1993) A glucose sensor based on graphite paste electrode modified with Tetracyanoquinodimethane. Indian J Chem 32:667–672
28. Pandey PC, Upadhyay S, Upadhyay BC, Pathak HC (1998) Ethanol biosensors and electrochemical oxidation of NADH. Anal Biochem 260:195–203. https://doi.org/10.1006/abio.1998.2679
29. Pandey PC, Upadhyay S, Pathak HC (1999) A new ferrocene-linked organically modified electrode sol-gel glass and its application in constructing Ion-selective electrodes. Electroanalysis 11:950–958
30. Pandey PC, Upadhyay S, Tiwari I, Sharma S (2001) A novel ferrocene encapsulated palladium-linked ormosil based electrocatalytic biosensor; role of reactive functional group. Electroanalysis 13(18):1519–1527
31. Pandey PC, Upadhyay S, Shukla NK, Sharma S (2003) Studies on the electrochemical performance of glucose biosensor based on ferrocene encapsulated ORMOSIL and glucose oxidase modified graphite paste electrode. Biosens Bioelectron 10:1257–1268. https://doi.org/10.1016/S0956-5663(03)00075-7
32. Pandey PC, Singh R, Pandey AK (2014) Tetrahydrofuran hydroperoxide and 3-Aminopropyltrimethoxysilanemediated controlled synthesis of Pd, Pd-Au, Au-Pd nanoparticles: role of Palladium nanoparticles on the redox electrochemistry of ferrocene monocarboxylic acid. Electrochimica Acta 138:163–173. https://doi.org/10.1016/j.electacta.2014.06.101
33. Pandey PC, Singh R (2015) Controlled synthesis of Pd, Pd-Au, nanoparticles; effects of organic amine and silanol groups on the morphology and polycrystallinity of nanomaterials. RSC Adv 5:10964–10973. https://doi.org/10.1039/C4RA16201C
34. Pandey PC, Pandey G, Haider J, Pandey G (2016) Role of organic carbonyl moiety and 3-aminopropyltrimethoxysilane on the synthesis of gold nanoparticles specific to pH and salt tolerance. J. Nanosci. Nanotechnol. 16:6155–6163. https://doi.org/10.1166/jnn.2016.11104
35. Kumar N, Rosy RN (2017) Goyal, Palladium nanoparticles decorated multi-walled carbon nanotubes modified sensor for the determination of 5-hydroxytryptophan in biological fluids. Sens Actuators B 239:1060–1068. https://doi.org/10.1016/j.snb.2016.08.122
36. Wu P, Huang Y, Zhao X, Lin D, Xie L, Li Z, Zhu Z, Lan M (2022) MnFe2O4/MoS2 nanocomposite as Oxidase-like for electrochemical simultaneous detection of ascorbic acid, dopamine and uric acid. Microchem J 181:107780. https://doi.org/10.1016/j.microc.2022.107780
37. Yang L, Liu D, Hunang J, You T (2014) Simultaneous determination of dopamine, ascorbic acid and uric acid at electrochemically reduced graphene oxide modified electrode. Sens Actuators, B Chem 193:166–172. https://doi.org/10.1016/j.snb.2013.11.104
38. Huang H, Yue Y, Chen Z, Chen Y, Wu S, Liao J, Liu S, Wen HR (2019) Electrochemical sensor based on a nanocomposite prepared from TmPO4 and graphene oxide for simultaneous voltammetric detection of ascorbic acid, dopamine and uric acid. Microchimia Acta 189:1–9. https://doi.org/10.1007/s00604-019-3299-7
39. Anan WK, Olarnwanich A, Sriprachuabwong C, Karuwan C, Tuantranont A, Wisitsoraat A, Srituravanich W, Pimpin A (2012) Disposable paper-based electrochemical sensor utilizing inkjet-printed polyaniline modified screen-printed carbon electrode for ascorbic acid detection. J Electroanal Chem 685:72–78. https://doi.org/10.1016/j.jelechem.2012.08.039
40. Chen W, Tang J, Cheng HJ, Xia XH (2009) A simple method for fabrication of sole composition nickel hexacyanoferrate modified electrode and its application. Talanta 80:539–543. https://doi.org/10.1016/j.talanta.2009.07.022
41. dos Santos PL, Katic V, Toledo KCF, Bonacin JA (2018) Photochemical one-pot synthesis of reduced graphene oxide/Prussian blue nanocomposite for simultaneous electrochemical detection of ascorbic acid, dopamine, and uric acid. Sens Actuators, B Chem 225:2437–2447. https://doi.org/10.1016/j.snb.2017.09.036
42. Ghanbari K, Hajheidari N (2015) ZnO–CuxO/polypyrrole nanocomposite modified electrode for simultaneous determination of ascorbic acid, dopamine, and uric acid. Anal Biochem 473:53–62. https://doi.org/10.1016/j.ab.2014.12.013

Authors and Affiliations

Kuldeep Kumar Maurya[1] · Kulveer Singh[1] · Manisha Malviya[1]

✉ Manisha Malviya
manisha.apc@iitbhu.ac.in

[1] Department of Chemistry, Indian Institute of Technology (BHU), Varanasi 221005, India